Development of two color laser diagnostics for the ITER poloidal polarimeter[a)]

K. Kawahata,[1,b)] T. Akiyama,[1] K. Tanaka,[1] K. Nakayama,[2] and S. Okajima[2]
[1]*National Institute for Fusion Science, 322-6 Oroshi-cho, Toki 509-529, Japan*
[2]*Chubu University, Matsumoto-cho, Kasugai-shi, Aichi 487-8501, Japan*

(Presented 17 May 2010; received 6 May 2010; accepted 10 June 2010; published online 29 October 2010)

Two color laser diagnostics using terahertz laser sources are under development for a high performance operation of the Large Helical Device and for future fusion devices such as ITER. So far, we have achieved high power laser oscillation lines simultaneously oscillating at 57.2 and 47.7 μm by using a twin optically pumped CH_3OD laser, and confirmed the original function, compensation of mechanical vibration, of the two color laser interferometer. In this article, application of the two color laser diagnostics to the ITER poloidal polarimeter and recent hardware developments will be described. © *2010 American Institute of Physics.* [doi:10.1063/1.3479119]

I. INTRODUCTION

Measurement of the plasma current density profile is indispensable for the so-called advanced modes of tokamak operation. In the International Thermonuclear Fusion Experimental Reactor (ITER), a poloidal polarimeter based on the Faraday effect of a far-infrared laser beam passing though the plasma has been designed[1] to measure the profile. A 118.8 μm CH_3OH laser line is proposed as a probing light source for the polarimeter, since the CH_3OH laser line is the shortest and high power far-infrared laser oscillation line among many oscillation lines applied on fusion devices so far. The Faraday rotation angles that can be expected in ITER are large enough to be measured accurately. However, the Cotton–Mouton effect is also large and should then be taken into account for evaluation of the rotation angle. Therefore, we have been developing shorter wavelength laser oscillation lines around 50 μm, since the Faraday rotation angle is still large enough and the Cotton–Mouton effect is small enough. Another advantage of adapting 50 μm is to reduce the beam bending effect to a quarter of that at 118.8 μm. We already achieved high power laser oscillation lines,[2] 57.2 and 47.7 μm, by using a CH_3OD laser optically pumped by the 9R(8) CO_2 laser line. These oscillation lines simultaneously oscillate with high power:[3] 1.6 W at 57.2 μm and 0.8 W at 47.7 μm. So far, we confirmed the usefulness of two color laser operation for vibration compensation[4] for interferometry in a test stand. For the measurement of the Faraday rotation angle, we have developed a photoelastic modulator[5] (PEM), operating around 50 μm, and performed bench tests of the polarimeter with dual PEMs and demonstrated the feasibility of the polarimeter. The achieved angular resolution[6] is 0.01° with a time resolution of 1 ms, which satisfies diagnostic requirements for q-profile measurements on ITER (0.05° at 10 ms time resolution). In this paper, an overall design of the ITER polarimeter using two color laser oscillations is investigated.

II. OPTICAL LAYOUT OF POLARIMETER

Figure 1 shows a schematic drawing of the optical configuration of a polari-interferometer with a two color laser system. The main components of the system, including a twin optically pumped laser and detection system, are placed in the diagnostic room biologically shielded with thick concrete walls. Therefore, the laser beam has to propagate about 44 m to reach the tokamak.[1] There are two ideas for efficient laser beam transmission, an over-sized beam pipe system and a waveguide transmission system. In the Large Helical Device,[6] a dielectric waveguide of 40 m in length is used for a 118.8 μm CH_3OH laser interferometer,[7] since a waveguide system has precise mode matching, easy alignment, and long time stability. The transmission efficiency including five miter bends is about 90%. We already confirmed[8] sufficient transmission properties of a dielectric waveguide for the 57.2 μm CH_3OD laser beam in a test stand. In Fig. 1, a dielectric waveguide of 47 mm in diameter is adopted. The probe beam is divided into many probe beams (15 channels in Ref. 1) and a reference beam by beam splitters made of highly resistive silicon. Highly resistive silicon is a low absorption material (absorption coefficient α=0.56 cm^{-1} at 47.7 μm) in short wavelength far-infrared (FIR) regime compared with quartz (α_o, α_e=6.6 cm^{-1}, 4.9 cm^{-1} at 47.7 μm). Each probe beam is led to the waveguide and port plugs with a free space propagation mode, injected into the plasma via a focusing mirror, and then reflected back with a corner cube retroreflector. The reflected beam goes back to the diagnostic room through the same waveguide, and finally is divided into two parts, Faraday rotation measurement with dual PEMs (PM1 and PM2) and phase shift measurement with heterodyne detection. In the polarimeter part, one wavelength is selected by the use of a Fabry–Pérot filter (FPF) for the measurement of a rotation angle of a selected wave-

[a)]Contributed paper, published as part of the Proceedings of the 18th Topical Conference on High-Temperature Plasma Diagnostics, Wildwood, New Jersey, May 2010.
[b)]Electronic mail: kawahata@lhd.nifs.ac.jp.

 © 2010 American Institute of Physics

Downloaded 02 Feb 2012 to 133.75.110.124. Redistribution subject to AIP license or copyright; see http://rsi.aip.org/about/rights_and_permissions

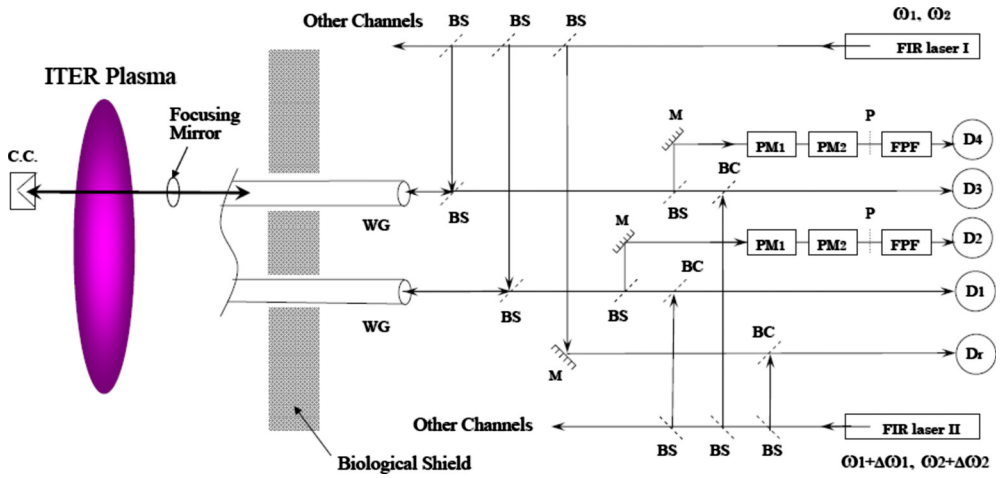

FIG. 1. (Color online) Schematic drawing of the polari-interferometer with the two color laser system. BS: beam splitter; BC: beam combiner; M: mirror; WG: waveguide; C.C.: corner cube retroreflector; PM: photoelastic modulator; FPF: Fabry–Pèrot filter; and D: detector.

length. A metal mesh (1000/in. and a wire width of 7.37 μm with the thickness of 5 μm) is adopted as a reflector for the FPF. The calculated reflectance of the mesh is 82% and the measured one is 86% at 57.2 μm. The measured transmission efficiency of the FPF was 65% at 57.2 μm.

Figure 2 shows the calculated beam waists of the full optical system from the retro-reflector up to the waveguide which is installed just outside the vacuum windows. The inner diameter of the input of the waveguide is 47 mm and beam radius at the waveguide is 15.7 mm for both laser beams. A focusing mirror with a focal length of 5.5 m is used to define the optimum beam waist at the position of the retroreflector. The radius of the beam waist is 6.4 mm for 57.2 μm and 5.3 mm for 47.7 μm at the position of the retroreflector. After reflecting back to the waveguide, the beam waists of both laser beams are almost the same (15.8 mm) as the original ones at the position of the waveguide. Optimum matching of the Gaussian beam into the waveguide via a spherical mirror installed in the port plug is expected.

In the optical configuration of Fig. 1, the incident beam

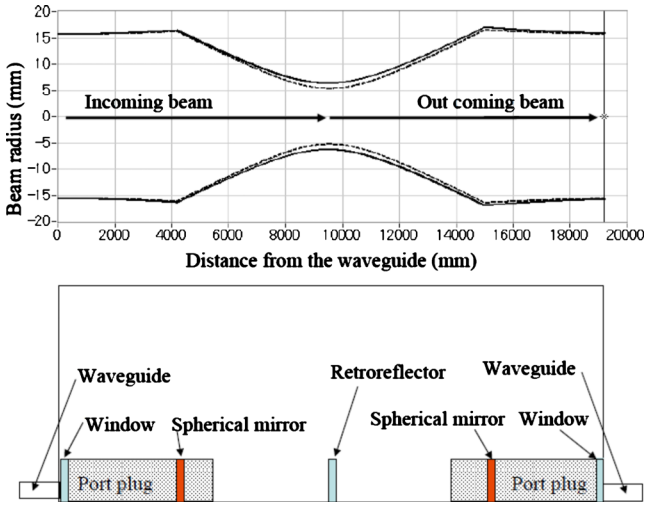

FIG. 2. (Color online) Calculated beam waist of the optical system from the retroreflector to the waveguide which is placed just outside of the vacuum window. Solid line: 57.2 μm; dotted line: 47.7 μm.

to the plasma is refracted due to the density gradient; hence, the incident angle of the reflected beam to the waveguide is deviated from the original one before the plasma production. In the ITER standard plasma operation $[n_e(\rho)=1\times10^{20}(1-\rho^8)\ m^{-3}]$, the typical refraction angle of CH.5 chord in Ref. 1 is estimated to be 0.01°. In order to examine the effect of refraction on matching the beam to the waveguide, transmission measurements have been carried out by using a dielectric waveguide (24 mm in diameter and 8.9 m length) with two miter bends. Figure 3 shows horizontal and vertical beam mode profiles of a 57.2 μm laser beam, which were measured with a pyroelectric detector attached on a motorized two-dimensional stage after passing through the dielectric wave guide at a distance of 3.1 m. In this experiment, the incidence angle to the WG was tilted by 0°, 0.035°, and 0.173°. The incident angle θ is defined as the angle between the beam axis and the waveguide axis. As the incident angle becomes large, the peak of the profile is shifted and a side lobe of the beam appears. Under the ITER diagnostic condition ($\theta\sim0.01°$), it is found that there are no large distortions of the laser beam transmission through the waveguide. A full size test stand except the waveguide length is under construction to simulate ITER diagnostics.

III. TWO COLOR LASER DIAGNOSTICS

In order to investigate diagnostic performance of the two color system, we have constructed a test stand[8] with the configuration of Michelson interferometer type, where effects of the mechanical vibration on the polari-interferometer are investigated. To simulate mechanical vibration a reflecting mirror of the interferometer is modulated. Figure 4(a) shows the vibrational displacements of the reflecting mirror evaluated from 57.2 and 47.7 μm interferometers. Frequencies of the added vibrations are 3, 140, and 300 Hz. The former low frequency is added by a vibrating mirror driver by a piezoelectric transducer. The latter two high frequencies are added by hitting the mirror by a tool intermittently. The subtracted signal between two wavelengths shows there is no low frequency component corresponding to the vibrations. As is shown in Fig. 4(b), high frequency noise is also well can-

Downloaded 02 Feb 2012 to 133.75.110.124. Redistribution subject to AIP license or copyright; see http://rsi.aip.org/about/rights_and_permissions

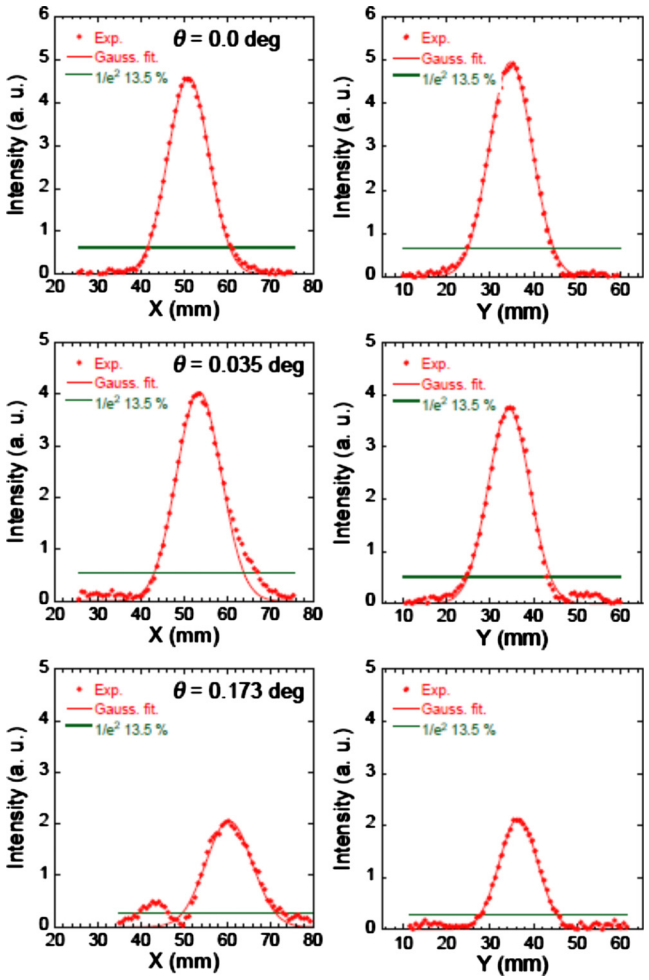

FIG. 3. (Color online) Horizontal and vertical beam mode profiles of a 57.2 μm laser beam after passing through the dielectric wave guide of 8.9 m in length with two miter bends. The incident angle θ to the WG was changed.

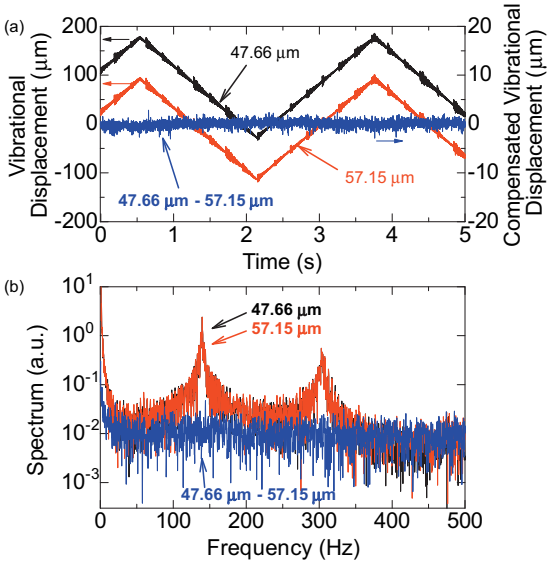

FIG. 4. (Color) Sample (a): The vibrational displacements of 57/48 μm interferometers and the vibration compensation with them. Frequencies of added vibrations are 3, 140, and 300 Hz. (b) Noise spectra of each interferometer and the vibration-compensated signal.

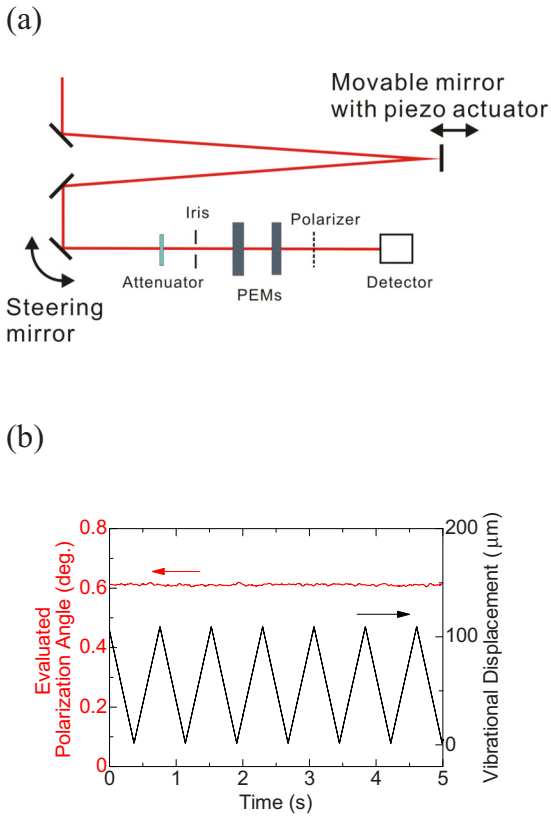

FIG. 5. (Color online) (a) Optical setup for tests of how the mechanical vibrations affect the measurement. (b) The evaluated polarization angle when the optical path length changes by a distance of 110 μm.

celled out. At the present, the uncompensated noise level of about 0.6 μm, which is thought to be caused by the detector noise or laser oscillation noise, corresponds to the line averaged electron density error of 4×10^{17} m^{-3} in ITER. Polarimetry is thought to be intrinsically immune to the mechanical vibrations. However, it slightly suffers side-effects depending on the measurement method and the direction of the vibration.[9] In order to examine the immunity to the mechanical vibrations of the polarimeter with PEMs, one of the mirrors is vibrated along the optical path as illustrated in Fig. 5(a). The vibration component is not observed in the evaluated polarization angle α as demonstrated in Fig. 5(b). The bending effect of a probe beam by a plasma may change the incident angle to the PEM. Simulation of such a situation by tilting a steering mirror in Fig. 5(a) indicates that a change in incident angle into the PEM $\Delta\theta$ of 1° leads to an error of the polarization angle $\Delta\alpha$ of about 1°. The maximum refraction angle due to the density gradient $[1\times10^{20}(1-\rho^8)$ $m^{-3}]$, which is estimated from the calculation in Ref. 1, is about 0.01°. Hence, the error from the beam bending effect is smaller than the target resolution 0.05° in ITER.

ACKNOWLEDGMENTS

This work was supported in part by a Grant-in-Aid for Science Research from the Japanese Ministry of Education, Culture, Sports, Science and Technology, "Priority area of Advanced Burning Plasma Diagnostics" (Grant No. 16082208) and also by the NIFS budget code of NIFS06ULHH501.

Downloaded 02 Feb 2012 to 133.75.110.124. Redistribution subject to AIP license or copyright; see http://rsi.aip.org/about/rights_and_permissions

[1] A. J. H. Donné, M. F. Graswinckel, M. Cavinato, L. Giudicotti, E. Zilli, C. Gil, H. R. Koslowski, P. McCarthy, C. Nyhan, S. Prunty, M. Spillane, and C. Walker, Rev. Sci. Instrum. **75**, 4694 (2004).
[2] S. Okajima, K. Nakayama, H. Tazawa, K. Kawahata, K. Tanaka, T. Tokuzawa, Y. Ito, and K. Mizuno, Rev. Sci. Instrum. **72**, 1094 (2001).
[3] K. Nakayama, H. Tazawa, S. Okajima, K. Kawahata, K. Tanaka, T. Tokuzawa, and Y. Ito, Rev. Sci. Instrum. **75**, 329 (2004).
[4] K. Kawahata, T. Akiyama, R. Pavlichenko, K. Tanaka, T. Tokuzawa, Y. Ito, S. Okajima, K. Nakayama, and K. Wood, Rev. Sci. Instrum. **77**, 10F132 (2006).
[5] T. Akiyama, K. Kawahata, S. Okajima, K. Nakayama, and T. C. Oakberg, J. Plasma Fusion Res. **2**, S1113 (2007).
[6] A. Komori, H. Yamada, S. Sakakibara, O. Kaneko, K. Kawahata, T. Mutoh, N. Ohyabu, S. Imagawa, K. Ida, Y. Nagayama, T. Shimozuma, K. Y. Watanabe, T. Mito, M. Kobayashi, K. Nagaoka, R. Sakamoto, N. Yoshida, S. Ohdachi, N. Ashikawa, Y. Feng, T. Fukuda, H. Igami, S. Inagaki, H. Kasahara, S. Kubo, R. Kumazawa, O. Mitarai, S. Murakami, Yuji Nakamura, M. Nishiura, T. Hino, S. Masuzaki, K. Tanaka, K. Toi, A. Weller, M. Yoshinuma, Y. Narushima, N. Ohno, T. Okamura, N. Tamura, K. Saito, T. Seki, S. Sudo, H. Tanaka, T. Tokuzawa, N. Yanagi, M. Yokoyama, Y. Yoshimura, T. Akiyama, H. Chikaraishi, M. Chowdhuri, M. Emoto, N. Ezumi, H. Funaba, L. Garcia, P. Goncharov, M. Goto, K. Ichiguchi, M. Ichimura, H. Idei, T. Ido, S. Iio, K. Ikeda, M. Irie, A. Isayama, T. Ishigooka, M. Isobe, T. Ito, K. Itoh, A. Iwamae, S. Hamaguchi, T. Hamajima, S. Kitajima, S. Kado, D. Kato, T. Kato, S. Kobayashi, K. Kondo, S. Masamune, Y. Matsumoto, N. Matsunami, T. Minami, C. Michael, H. Miura, J. Miyazawa, N. Mizuguchi, T. Morisaki, S. Morita, G. Motojima, I. Murakami, S. Muto, K. Nagasaki, N. Nakajima, Y. Nakamura, H. Nakanishi, H. Nakano, K. Narihara, A. Nishimura, H. Nishimura, K. Nishimura, S. Nishimura, N. Nishino, T. Notake, T. Obana, K. Ogawa, Y. Oka, T. Ohishi, H. Okada, K. Okuno, K. Ono, M. Osakabe, T. Osako, T. Ozaki, B. J. Peterson, H. Sakaue, M. Sasao, S. Satake, K. Sato, M. Sato, A. Shimizu, M. Shiratani, M. Shoji, H. Sugama, C. Suzuki, Y. Suzuki, K. Takahata, H. Takahashi, Y. Takase, Y. Takeiri, H. Takenaga, S. Toda, Y. Todo, M. Tokitani, H. Tsuchiya, K. Tsumori, H. Urano, E. Veshchev, F. Watanabe, T. Watanabe, T. H. Watanabe, I. Yamada, S. Yamada, O. Yamagishi, S. Yamaguchi, S. Yoshimura, T. Yoshinaga, and O. Motojima, Nucl. Fusion **49**, 104015 (2009).
[7] K. Kawahata, K. Tanaka, Y. Ito, A. Ejiri, and S. Okajima, Rev. Sci. Instrum. **70**, 707 (1999).
[8] K. Kawahata, T. Akiyama, K. Tanaka, K. Nakayama, and S. Okajima, Rev. Sci. Instrum. **79**, 10E707 (2008).
[9] T. Akiyama, S. Tsuji-Iio, R. Shimada, K. Nakayama, S. Okajima, M. Takahashi, K. Terai, K. Tanaka, T. Tokuzawa, and K. Kawahata, Rev. Sci. Instrum. **74**, 2695 (2003).

Downloaded 02 Feb 2012 to 133.75.110.124. Redistribution subject to AIP license or copyright; see http://rsi.aip.org/about/rights_and_permissions